



Dynamic Behavior of Primary Cilia During Cellular Migration

Kazuyuki Matsushima^a, Kuniyoshi Kaseda^{b*}

^{a,b}*Saravio Central Institute, Saravio Cosmetics Ltd., 1356-6 Oaza Tsurumi, Beppu, Oita 874-0840, Japan*

^a*Email: matsushima@saravio.jp*

^b*Email: kaseda@saravio.jp*

Abstract

Dermal papilla cells (DPCs) play pivotal roles in hair follicle development and repetitive hair growth cycles, in which cellular migration is deeply involved. We previously suggested that primary cilia of DPCs regulate the hair follicle physiologies via intercellular signal transduction. However, the role of the primary cilia in cell migration has yet to be addressed. Here, immunofluorescence microscopic observations revealed that primary cilia of DPCs predominantly protruded toward the backward direction in the initial phase of cellular migration, while the organelle of non-migrating cells oriented randomly. In addition, the average length of the primary cilia became shorter upon the onset of the active motion, compared to those in multicellular spheroids. Moreover, the appearance frequency was dramatically decreased in migrating cells. Similar results were obtained using human dermal fibroblasts and articular synoviocytes. Collectively, our current findings suggest that those fibroblastic cells set the primary cilia to the backward direction in the initial phase of migration, along with the tuning of the length and appearance frequency of the sensory organelle. These regulations should be essential for proper cellular migration in tissue developments and wound-healing processes.

Keywords: Dermal fibroblast; dermal papilla cell; synoviocyte; migration; primary cilium; spheroid; wound healing.

* Corresponding author.

1. Introduction

Spatial and temporal rearrangements of cellular components repeatedly take place in self-renewing hair follicles. Mesenchyme-derived dermal papilla cells (DPCs) regulate other cells through intercellular signal transduction at the base of the hair follicles [1]. In the hair growth phase (anagen), DPCs promote the proliferation and differentiation of epidermal cells. At the onset of regression phase (catagen), a subset of DPCs actively emigrates out of the dermal papilla and the cells reintegrate in dermal sheath cups underneath [2,3]. In the resting phase of the hair cycle (telogen), a new population of DPCs is prepared from hair follicle dermal stem cells. When the progenitor cells migrate into the dermal papilla, the next hair growth cycle starts [3,4]. Therefore, the number of the cells in the dermal papillae varies during the hair growth cycle, where cellular migration plays an essential role [2–4]. In addition, the mesenchymal fibroblast-like cells migrate toward epidermal placode to establish dermal condensates (DPC aggregates) in the process of hair follicle formation [5]. Cellular migration of DPCs widely plays pivotal roles in hair follicle physiology.

A microtubule-based primary cilium functions as a signaling center in mammalian cells. According to the previous report, mice showed severe lack of hair when primary cilia of dermal cells were disrupted [6]. We recently demonstrated that the primary cilium of DPCs is involved in the regulation of intercellular signaling, thereby, in the proliferation activity of other cells [7]. In addition, the antenna-like organelle plays a key role in directional migration and chemotaxis [8,9]. The majority of the previous studies described that primary cilia are reoriented in parallel to the direction of the cellular movement [8–10], while a few studies showed random directions of the organelle during the migration process [11,12]. L. Schneider and his colleagues (2010) reported that the primary cilia protrude predominantly toward the forward direction of migrating cells [13]. The authors additionally stated that the primary cilia occasionally orient backward, i.e., pointing toward the trailing edge of the cells. However, quantitative analysis, in relation to the orientation of the organelle, was not described, despite of an ingenious mechanism of PDGF-AA-based chemotaxis. No other studies have addressed the intriguing question of the direction of the organelle during cellular migration process.

In the current work, we quantitatively investigated primary cilia of three different types of fibroblastic cells, by simultaneous observations of the basal bodies at the origin of the organelle of interest. Here we describe that the primary cilia predominantly incline toward the backward direction in the initial phase of cellular migration. In addition, the migrating cells show the reduced length of primary cilia with the lower appearance frequency.

2. Materials and methods

2.1. Cell culture

Primary human DPCs from Caucasian females were purchased from PromoCell (Heidelberg, Germany). The cells were maintained as described previously [7]. Primary dermal fibroblasts (DFs) were purchased from Cell Applications Inc. (San Diego, CA, USA). Primary human fibroblast-like synoviocytes (FLSs) were a gift from Dr. S. Miyaki (Hiroshima University, Japan). Spheroidal multicellular clusters of DPCs were prepared using ultra-low-attachment plates (Corning Inc., NY, USA), as described previously [14]. For gap-filling experiments, DPCs were seeded on a collagen-coated glass (2×10^5 cells/well), and the cells were grown to confluence. After

incubating the cells with starving medium containing 0.1% fetal calf serum for 24 hrs, a scratch was made by running a pipette tip over the confluent monolayer, as described previously [14].

2.2. Primary cilia imaging

Immunofluorescent staining of primary cilia was performed as described previously [7], using a mouse anti-acetylated α -tubulin antibody (clone 6-11B-1; Sigma-Aldrich, St Louis, MO, USA; 1:5,000 dilution) and a basal body marker (rabbit polyclonal anti- γ -tubulin antibody, T3559; Sigma-Aldrich, St Louis, MO, USA; 1:5,000 dilution). For spheroid-based experiments, the cells were fixed with 4% paraformaldehyde after 16 hrs incubation on a collagen-coated glass. For gap-filling experiments, the cells were fixed 8 or 16 hrs after a scratch was made.

2.3. Measurements of the migration distance and the primary cilium angle

In order to measure migration distance (Δ_1) in spheroid-based experiments, we first defined the edge of a spheroid, as a boundary line between cell-occupied and cell-free regions (Figure 1A). The migration distance was measured as the distance between the basal body and the edge of the spheroid. The angles between the ciliary axis and the perpendicular line from the basal body to the center of the spheroid (the primary cilium angle, θ_1), were measured, regardless of clockwise or counter-clockwise direction. Therefore, the angles are distributed between 0° and 180° . In gap-filling experiments, the primary cilium angle (θ_2) was defined as the angle between the ciliary axis and the perpendicular line from the basal body to the edge of the initial gap (Figure 1B). Both the migration distances and the primary cilium angles were analyzed using an ImageJ software (US National Institutes of Health).

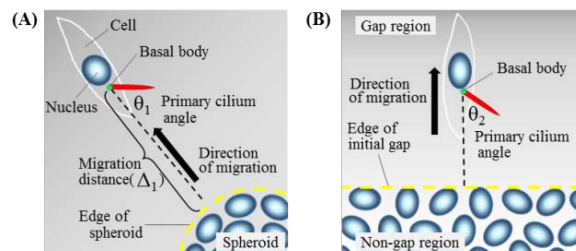


Figure 1: Schematic illustrations of measurements. The migration distance (Δ_1) and the primary cilium angles (0° to 180°) were measured in spheroid-based assays (A) and in gap-filling assays (B). The primary cilia and basal bodies are shown by red poles and green circles, respectively. The migration displacement is defined as distance between the basal body and the closest edge of the surfaces of the cellular aggregation (spheroid or the initial gap). The θ value are determined as angles between the ciliary axis and the perpendicular line from the basal body to the edge of the spheroid or the initial gap.

2.4. Statistical analysis

All experiments were repeated at least three times. The data are presented as mean \pm SE. Statistical analysis was performed using a Kaleidagraph software (Synergy Software, Reading, PA, USA). For primary cilia length,

non-parametric statistical analysis (Mann–Whitney U test) was conducted. In the other analysis, a two-tailed approach was used. Heat map graphs were created by using the heat map module of a statistical software (R, version 3.3, <https://cran.r-project.org/>). *P* values of less than 0.05 were considered statistically significant.

3. Results

In order to examine the direction, the length and the appearance frequency of the primary cilia of migrating DPCs, we first prepared multicellular spheroids using ultra-low-attachment plates [14]. When the microspheres were transferred onto collagen-coated surfaces, spindle-shaped cells started to migrate away from the spheroids. As shown in Figure 2A, the primary cilia protruded backward, toward the spheroid. We measured primary

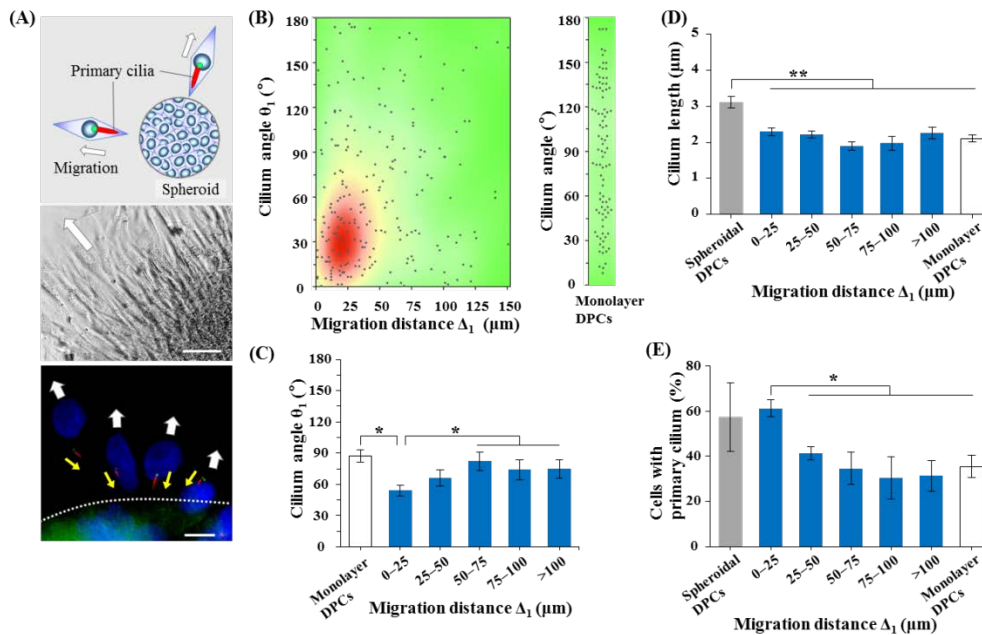


Figure 2: Direction, length and appearance frequency of primary cilia in DPCs in spheroid assays. (A) Top, a schematic illustration of DPCs migrating out of a spheroid. Red poles and green circles show primary cilia and basal bodies, respectively. The arrows show the direction of cellular movement. Middle, a phase-contrast image of spindle-shaped migrating cells from a microsphere. Scale bar =100 μm . Bottom, immunocytochemistry of the primary cilia in DPCs migrating out of spheroids. Anti-acetylated α -tubulin (red), anti- γ -tubulin (green) antibodies and Hoechst 33342 dye (blue) were used to visualize primary cilia, basal bodies and nuclei, respectively. A dotted line represents the edge of the spheroid, as a boundary line between cell-occupied and cell-free regions. The white arrows show the direction of cellular movement. The yellow arrows represent the orientation of primary cilia. Scale bar =10 μm . (B) Heat-mapped correlation between the migration distance (Δ_1) and the primary cilium angle (θ_1). The angle of primary cilia are distributed in a biased manner for migrating cells (left) and in an even manner for monolayer cells (right). Gray spots show individual data ($n > 100$ primary cilia). (C) The averaged θ_1 for DPCs migrating from spheroids (blue bars) and monolayer DPCs (white bar), respectively. (D, E) The average length and the appearance frequency of primary cilia during migration (blue bars). 100–200 primary cilia were analyzed for each group. Results of spheroidal and monolayer DPCs are shown in a gray and a white bar, respectively. * and ** indicate *P*-values < 0.05 and 0.01 , respectively.

cilium angles (θ_1) and migration distance (Δ_1), as described in Materials and Methods. The analysis showed that the angles were distributed predominantly in acute values ($0-60^\circ$), especially when migration distances were less than $50\ \mu\text{m}$ (red area in Figure 2B). The quantitative result clearly demonstrates that the majority of the primary cilia of DPCs point toward the spheroid, i.e., the backward direction of the cellular movement, in the initial phase of migration. Interestingly, as DPCs migrated further over $50\ \mu\text{m}$, the angles were distributed broadly, resulting in the significantly higher values of the averaged θ_1 . Similar random distribution of primary cilia was observed in monolayer DPCs (Figure 2B and C).

In order to further examine whether cellular migration affects the dynamics of primary cilia, the length and the appearance frequency of the organelle were quantified (Figure 2D and E). The average length of the primary cilia in the spheroidal DPCs was $3.1 \pm 0.2\ \mu\text{m}$, which is in good agreement with our previous report [7]. Upon the initiation of migration, primary cilia became shorter to around $2\ \mu\text{m}$, which is similar to monolayer DPCs (Figure 2D). Although the appearance frequency of the primary cilia in the range of $0-25\ \mu\text{m}$ distance was similar to that of spheroidal DPCs, the frequency were gradually decreased to the level of monolayer DPCs as the cells migrated further (Figure 2E). These results indicate that primary cilia are disassembled during the cellular migration process.

To rule out the possibility that the above observations are limited in the spheroid-based experimental condition, we repeated the analysis in standard gap-filling experiments (Figure 3). When a scratch was made in the confluent DPCs, the cells began to move toward the gap region (Figure 3A). At 8 hrs after scratching, most of the migrating cells were observed within $100\ \mu\text{m}$ from the edge of the initial gap. We measured the angles of the primary cilia (θ_2) in those cells, as shown in Figure 1B. The angles were distributed broadly in the non-gap region (Figure 3B). The average angle and the median value were $92 \pm 6^\circ$ and 97° , respectively. The result indicates that primary cilia orient in all directions in non-gap area. In contrast, the θ_2 distribution were highly biased toward the lower angles in the gap region of under $50\ \mu\text{m}$ distance, with the average angle and the median value of $60 \pm 7^\circ$ and 33° , respectively. The θ_2 distribution became broader in the gap region of over $50\ \mu\text{m}$ distance, with the average angle and the median value of $85 \pm 6^\circ$ and 77° , respectively, which is similar to the values of monolayer DPCs (the average angle and the median value were $87 \pm 6^\circ$ and 97° , respectively). These results confirmed that the primary cilia predominantly protrude toward the trailing edge of the migrating cells in the early phase of migration. Similar to the spheroidal assay, the length and the appearance frequency of the primary cilia in the migrating cells became shorter and lower, respectively, toward the levels of monolayer DPCs (Figure 3C and D).

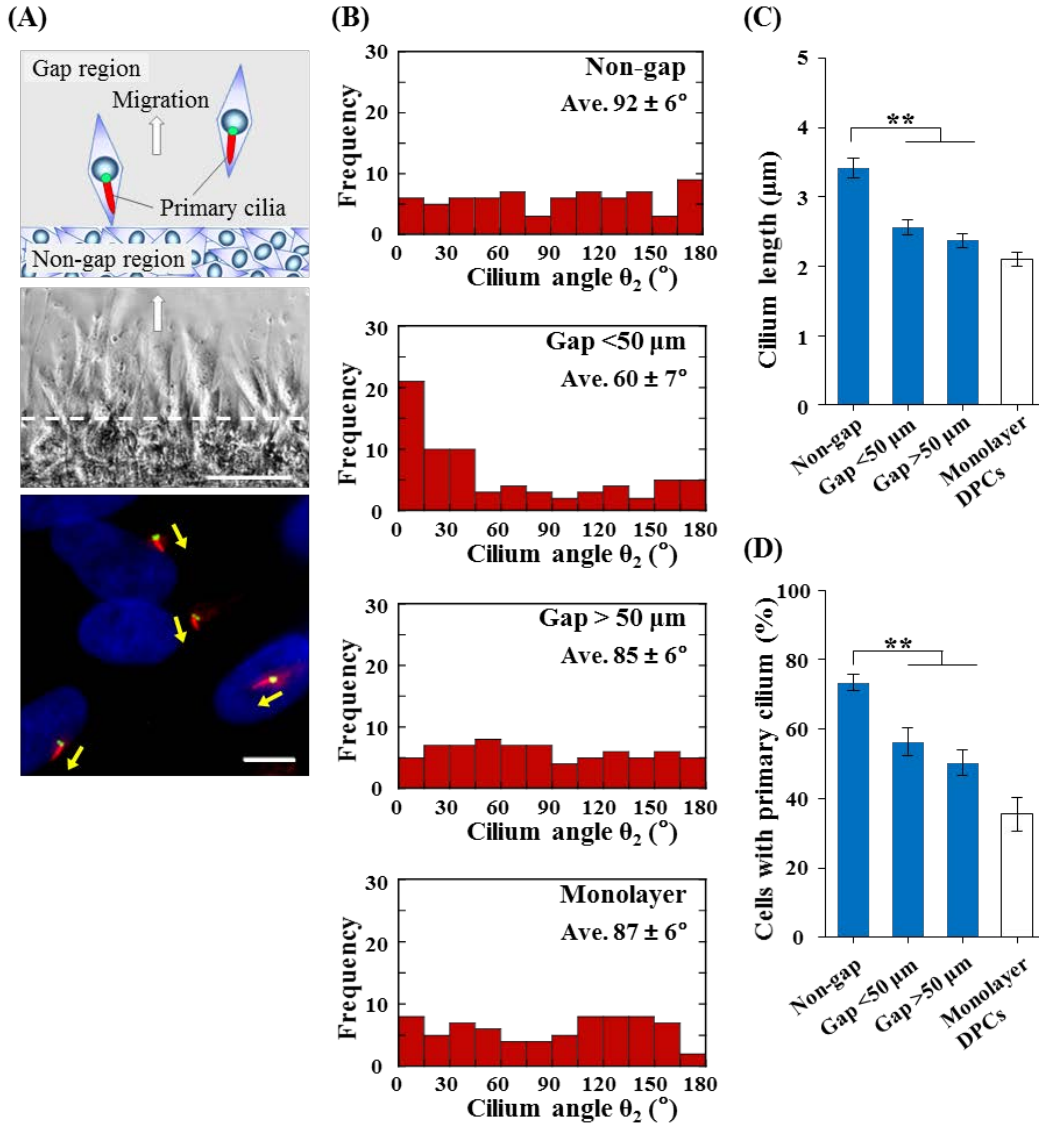


Figure 3: Direction, length and appearance frequency of primary cilia in DPCs in gap-filling assays. (A) Top, a schematic illustration of DPCs migrating into a gap region. Red poles and green circles show primary cilia and basal bodies, respectively. The arrow shows the direction of cellular movement. Middle, a phase-contrast image of spindle-shaped migrating cells from a non-gap region. The edge of the initial gap is represented by a dashed line. Scale bar = 100 μm . Bottom, immunocytochemistry of primary cilia in DPCs migrating upward into the gap region. Anti-acetylated α -tubulin (red), anti- γ -tubulin (green) antibodies and Hoechst 33342 dye (blue) were used to visualize primary cilia, basal bodies and nuclei, respectively. The yellow arrows represent the orientation of primary cilia. Scale bar = 10 μm . (B) Histograms of primary cilium angle (θ_2) of DPCs in the non-gap region, the gap regions and monolayered culture. The angles were highly biased into acute angles in the gap area of less than 50 μm from the edge of the initial boundary. Even distribution is observed when the cells migrate more than 50 μm . The angles are also evenly distributed both in the non-gap region (top) and in monolayered culture (bottom). The length (C) and the appearance frequency (D) of primary cilia. More than 100 primary cilia were analyzed in each region. The both parameters decrease upon the initiation of cellular migration, toward the level of monolayer cells. Non-gap, cells in non-gap regions; Gap $< 50 \mu\text{m}$, migrating cells less than 50 μm from the edge of the initial gap; Gap $> 50 \mu\text{m}$, migrating cells more than 50 μm from the edge of the initial gap; Monolayer, cells grown to around 50% confluence. ** indicates P-value < 0.01 .

In order to examine whether the morphological regulations of primary cilia are common in migrating cells, we further performed the gap-filling experiments using other primary human cells, dermal fibroblasts (DFs) and articular fibroblast-like synoviocytes (FLSs) as shown in Figure 4 and 5, respectively. Similar to DPCs, the

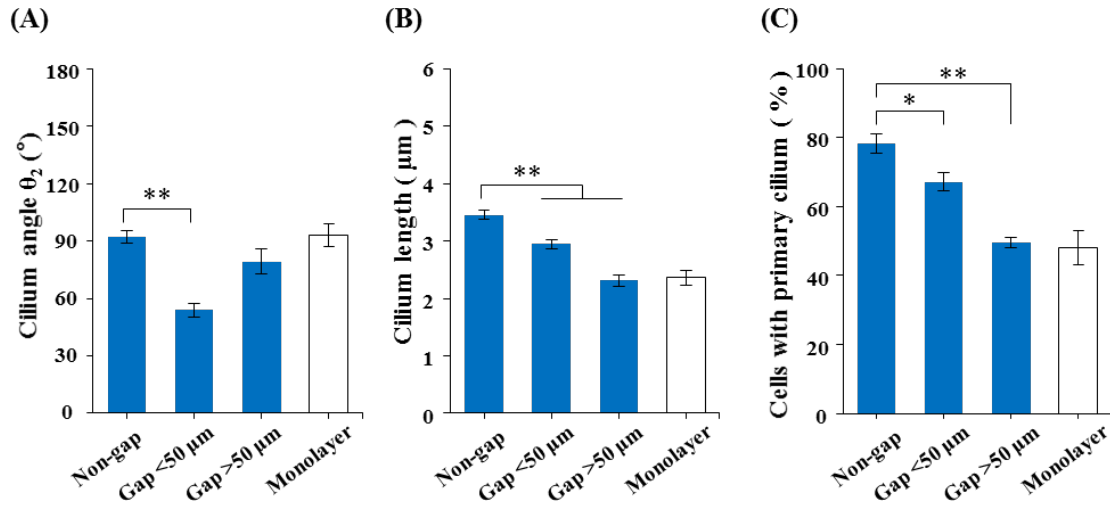


Figure 4: Direction, length and appearance frequency of primary cilia in human DFs in gap-filling assays. The direction (A), the length (B) and the appearance frequency (C) of primary cilia in primary human DFs. More than 100 primary cilia were analyzed for each group. Non-gap, cells in non-gap regions; Gap <50 μm , migrating cells less than 50 μm from the edge of the initial gap; Gap >50 μm , migrating cells more than 50 μm from the edge of the initial gap; Monolayer, cells grown to around 50% confluence. * and ** indicate P-values < 0.05 and 0.01, respectively.

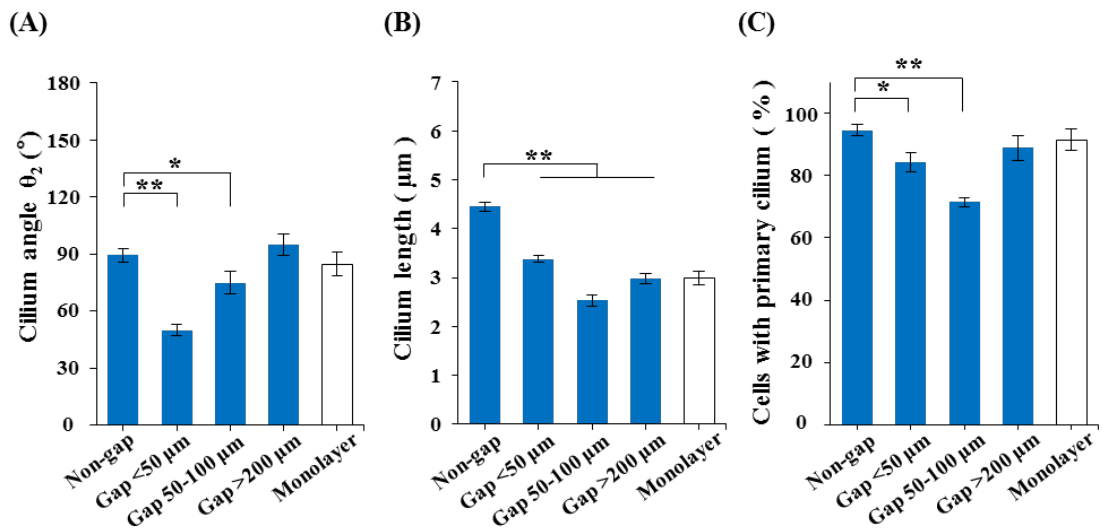


Figure 5: Direction, length and appearance frequency of primary cilia in human FLSs in gap-filling assays. The direction (A), the length (B) and the appearance frequency (C) of primary cilia in primary human FLSs. Data were categorized and labeled in the same way as described in the legend of Figure 4. More than 100 primary cilia were analyzed for each group. * and ** indicate P-values < 0.05 and 0.01, respectively.

primary cilia of these cells protruded toward the backward direction of the cellular movement in the gap regions of under 50 μm distance ($54 \pm 4^\circ$ and $50 \pm 3^\circ$ for DFs and FLSs, respectively), while the organelle pointed randomly in the non-gap regions ($92 \pm 4^\circ$ and $89 \pm 4^\circ$ for DFs and FLSs, respectively). When the cells migrated further away, the θ_2 values became higher, toward the levels of monolayer cells. In addition, both the length and the appearance frequency of the primary cilia in the gap region were decreased, compared to those in the non-gap region (Figure 4B, C, Figure 5B and C). Again, these values became closer to the levels of monolayer cells as the migration distance became longer in the both two different types of cells. Based on these results, we have concluded that the direction, the length and the appearance frequency of primary cilia are regulated in the same manner in the initial phase of cellular migration, at least, in the mesenchymal-derived fibroblastic cells.

4. Discussion

In this study, we quantitatively analyzed the primary cilia of mesenchymal-derived fibroblastic cells to demonstrate that the organelle inclines predominantly toward the backward direction of cellular movement at the initial stage. A migrating DPC could sense signaling factor(s) that are derived from spheroidal DPCs, via a primary cilium, since the cells produce the elevated level of signaling molecules upon the spheroid formation [15,16]. In other word, it is possible that the orientation of the sensory organelle is regulated by the intercellular communication with signaling factor(s). To test this hypothesis, pre-formed spheroids were introduced into the culture of monolayer DPCs and the orientation of primary cilia of the 2D cells nearby was examined (Figure 6).

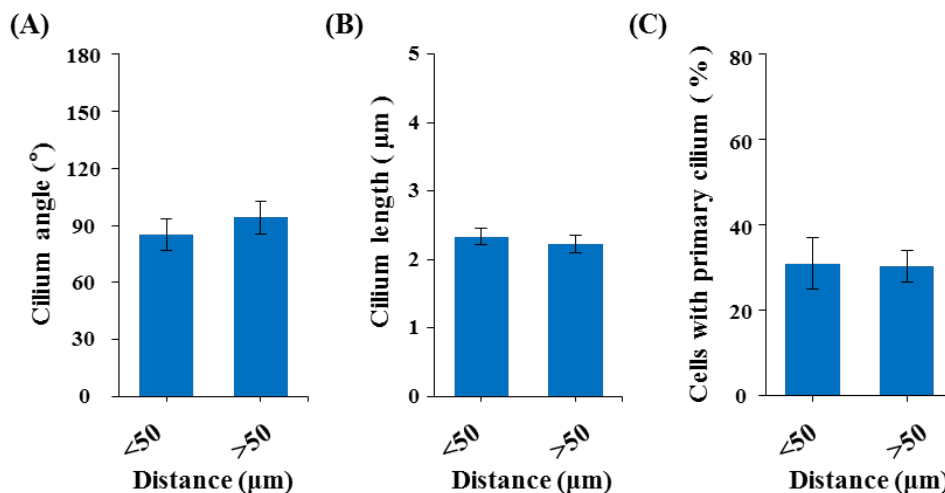


Figure 6: Migration process is a decisive factor for the dynamic behaviors of primary cilia. Pre-formed microspheres of DPCs were introduced onto two-dimensional cultures of the cells. Cilial angles of the monolayer cells around a spheroid are randomly distributed, regardless of the distance from spheroids (A). The length (B) and the appearance frequency (C) of the organelles are similar to the normal monolayer cells (see Figure 2).

In the case of the hypothesized scenario, those organelles would orient toward an introduced microsphere. Different from the hypothesis, however, the orientation of the primary cilia was random, which is similar to the distribution of normal monolayer cells (the average angle and the median value, $85 \pm 8^\circ$ and 77° , respectively). In addition, the length and the appearance frequency of primary cilia in this assay were not distinguished from

those in the normal 2D assay (see Figure 2C–E). These results indicate that not a signaling molecule from spheroidal DPCs but the migration process decides the orientation of the organelle. However, we still cannot rule out the possibility that specific molecule(s) affects the cilial orientation only during cellular migration. Therefore, we investigated the effect of PDGF-AA on the orientation of primary cilia of migrating cells in the spheroid assay. It was shown that PDGF-AA navigates the directional migration of fibroblasts [13]. Provided that PDGF-AA is involved in the orientation of primary cilia in our assays, excess signaling molecules in the culture media shall disturb the biased distribution of the cilial angles. In the presence of PDGF-AA, the average angle θ_1 became slightly bigger by 8 %, from $65 \pm 7^\circ$ to $70 \pm 7^\circ$. The tendency of the increase implies the possible contribution of the signaling molecule(s) to the biased orientation of the sensory organelle. Further investigation is to be carried out for a better understanding of the molecular mechanism.

The previous reports, using a gap-filling assay, showed that microtubule-organizing centers containing basal bodies are re-positioned ahead of the nuclei in migrating cells [8,17]. In good agreement with the previous results, the further the cells migrated off the non-gap area, the more microtubule-organizing centers are re-positioned anteriorly to nucleus together with primary cilia, in all the cells tested (Figure 7). It is interesting to investigate the relationship between the re-positioning of microtubule-organizing centers and the dynamic behaviors of primary cilia, in line with the molecular regulation of basal bodies. A better understanding of the fine-tuning system of the tubulin-based dynamic machineries will throw a new light on the research field of cellular migration.

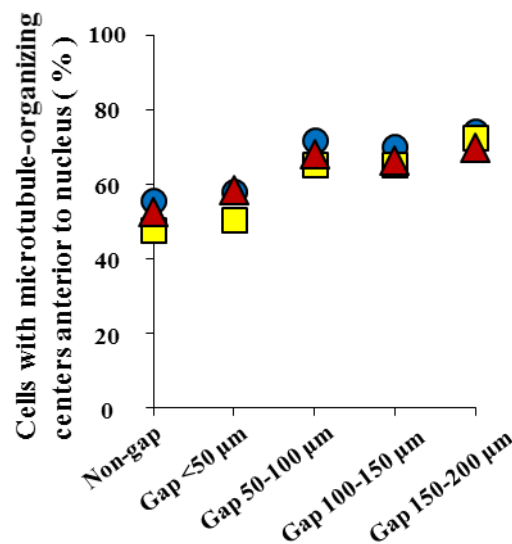


Figure 7: Re-positioning of microtubule-organizing centers during cellular migration. Microtubule-organizing centers are located in front of nuclei in a half population of the non-migrating cells. As the cells migrate further, the increased number of cells re-positions the cytoskeletal machinery anteriorly. Blue circles, DPCs; red triangles, DFs; yellow squares, FLSs.

We have recently described the mitochondrial conformational transition upon the initiation of cellular migration: the filamentous form dominates migrating DPCs, while the rounded form dominates spheroidal

DPCs [14,18]. Importantly, the extended filamentous mitochondria produce more cellular energy (ATP) than the other configuration, which is reasonable for the cells in order to perform the energy demanding migration. In our current model, DPCs make the primary cilia orientated toward the center of dermal papilla, at the beginning of catagen. The cells migrate out of quiescent dermal papilla toward dermal sheath cups, using filamentous mitochondria (Figure 8). During the migrating process, the angle, the length and the appearance frequency of primary cilia are dynamically regulated, along with re-positioning of microtubule-organizing centers. Further investigation of the collaborative system of primary cilia with other organelles/machineries will be beneficial for a further understanding of dynamic events such as hair growth cycle, wound healing and tissue development.

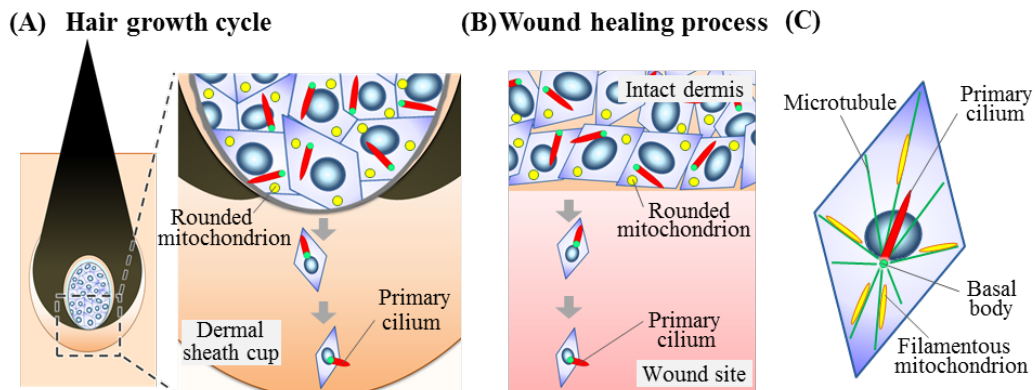


Figure 8: Proposed model. (A) At the beginning of the regression phase (catagen) of hair growth cycles, a subset of DPCs migrate out of the dermal papilla. Upon the initiation of the cellular movement, the cells reorient the primary cilia back toward the regulatory cockpit (upward) and the sensory organelle become shorter. At the same time, more ATP is produced by a rounded-filamentous conformational change of mitochondria. As DPCs travel further toward the dermal sheath cup (downward), the appearance frequency of primary cilia is reduced. These dynamic events of the organelles take place concomitantly with cytoskeletal rearrangement, including re-positioning of microtubule-organizing centers. (B) Similar re-arrangements of the tubulin-based structures and mitochondria take place in wound healing processes. (C) Schematic representation of organelles in a migrating cell.

5. Conclusion

We have demonstrated that the fibroblastic cells such as DPCs, FLSs and DFs set primary cilia to the backward direction in the initial phase of migration, along with the tuning of the length and the appearance frequency of the sensory organelle. Direct roles of primary cilia, in hair growth cycle, wound healing and tissue development, shall be investigated.

6. Recommendations

Our current findings will give a great impact to not only cell biologists but also medical scientists since both primary cilia and cellular migration are tightly relevant to physiological/medical issues.

Conflict of interest

The authors declare no conflict of interest associated with this manuscript.

Funding

This research did not receive any specific grant from funding agencies in the public, commercial, or not-for-profit sectors.

Authors' contributions

KK designed and supervised the research. KM performed the experiments. KM and KK wrote the manuscript. All authors have read and approved of the final version of the manuscript.

References

- [1]. B.A. Morgan. "The dermal papilla: an instructive niche for epithelial stem and progenitor cells in development and regeneration of the hair follicle." *Cold Spring Harb. Perspect. Med.*, vol. 4(7), a015180, 2014.
- [2]. D.J. Tobin, A. Gunin, M. Magerl, B. Handjiski, R. Paus. "Plasticity and cytokinetic dynamics of the hair follicle mesenchyme: implications for hair growth control." *J. Invest. Dermatol.*, vol. 120(6), pp. 895–904, 2003.
- [3]. W. Chi, E. Wu, B.A. Morgan. "Dermal papilla cell number specifies hair size, shape and cycling and its reduction causes follicular decline." *Development*, vol. 140(8), pp. 1676–83, 2013.
- [4]. W. Rahmani, S. Abbasi, A. Hagner, E. Raharjo, R. Kumar, A. Hotta, et al. "Hair follicle dermal stem cells regenerate the dermal sheath, repopulate the dermal papilla, and modulate hair type." *Dev. Cell*, vol. 31(5), pp. 543–58, 2014.
- [5]. S.E. Millar. "Molecular mechanisms regulating hair follicle development." *J. Invest. Dermatol.*, vol. 118(2), pp. 216–25, 2002.
- [6]. J.M. Lehman, E. Laag, E.J. Michaud, B.K. Yoder. "An essential role for dermal primary cilia in hair follicle morphogenesis." *J. Invest. Dermatol.*, vol. 129(2), pp. 438–48, 2009.
- [7]. K. Matsushima, M. Suematsu, C. Mifude, K. Kaseda. "Primary cilia-mediated intercellular signaling in hair follicles." *Integr. Mol. Med.*, vol. 3(3), pp. 699–702, 2016.
- [8]. T. Katsumoto, K. Higaki, K. Ohno, K. Onodera. "The orientation of primary cilia during the wound response in 3Y1 cells." *Biol. Cell*, vol. 81(1), pp. 17–21, 1994.
- [9]. T.J. Jones, R.K. Adapala, W.J. Geldenhuys, C. Bursley, W.A. AbouAlaiwi, S.M. Nauli, et al. "Primary

- cilia regulates the directional migration and barrier integrity of endothelial cells through the modulation of hsp27 dependent actin cytoskeletal organization." *J. Cell. Physiol.*, vol. 227(1), pp. 70–6, 2012.
- [10]. G. Albrecht-Buehler. "Phagokinetic tracks of 3T3 cells: parallels between the orientation of track segments and of cellular structures which contain actin or tubulin." *Cell*, vol. 12(2), pp. 333–9, 1977.
- [11]. N. Kumamoto, Y. Gu, J. Wang, S. Janoschka, K. Takemaru, J. Levine, et al. "A role for primary cilia in glutamatergic synaptic integration of adult-born neurons." *Nat. Neurosci.*, vol. 15(3), pp. 399–405, 2012.
- [12]. M. Pruski, A. Rajnicek, Z. Yang, H. Clancy, Y.Q. Ding, C.D. McCaig, et al. "The ciliary GTPase Arl13b regulates cell migration and cell cycle progression." *Cell Adh. Migr.*, vol. 10(4), pp. 393–405, 2016.
- [13]. L. Schneider, M. Cammer, J. Lehman, S.K. Nielsen, C.F. Guerra, I.R. Veland, et al. "Directional cell migration and chemotaxis in wound healing response to PDGF-AA are coordinated by the primary cilium in fibroblasts." *Cell. Physiol. Biochem.*, vol. 25(2–3), pp. 279–92, 2010.
- [14]. C. Mifude, K. Kaseda. "PDGF-AA-induced filamentous mitochondria benefit dermal papilla cells in cellular migration." *Int. J. Cosmet. Sci.*, vol. 37(3), pp. 266–71, 2015.
- [15]. M. Ohyama, T. Kobayashi, T. Sasaki, A. Shimizu, M. Amagai. "Restoration of the intrinsic properties of human dermal papilla in vitro." *J. Cell Sci.*, vol. 125(Pt 17), pp. 4114–25, 2012.
- [16]. C.A. Higgins, J.C. Chen, J.E. Cerise, C.A. Jahoda, A.M. Christiano. "Microenvironmental reprogramming by three-dimensional culture enables dermal papilla cells to induce de novo human hair-follicle growth." *Proc. Natl. Acad. Sci. U S A*, vol. 110(49), pp. 19679–88, 2013.
- [17]. C.J. Lu, H. Du, J. Wu, D.A. Jansen, K.L. Jordan, N. Xu, et al. "Non-random distribution and sensory functions of primary cilia in vascular smooth muscle cells." *Kidney Blood Press. Res.*, vol. 31(3), pp. 171–84, 2008.
- [18]. C. Mifude, K. Kaseda. "Shaping up mitochondrion in motion." *Dermatol. Open J.*, vol. 1(2), pp. 38–41, 2016.